Commun. Comput. Phys.
doi: 10.4208/cicp.111209.240710s

Vol. **11**, No. 2, pp. 351-366
February 2012

Conservative Finite-Difference Scheme for High-Frequency Acoustic Waves Propagating at an Interface Between Two Media

J. Staudacher and É. Savin*

ONERA – The French Aerospace Lab, F-92322 Châtillon, France.

Received 11 December 2009; Accepted (in revised version) 24 July 2010

Available online 24 October 2011

Abstract. This paper is an introduction to a conservative, positive numerical scheme which takes into account the phenomena of reflection and transmission of high frequency acoustic waves at a straight interface between two homogeneous media. Explicit forms of the interpolation coefficients for reflected and transmitted wave vectors on a two-dimensional uniform grid are derived. The propagation model is a Liouville transport equation solved in phase space.

AMS subject classifications: 35L45, 65M06, 65M12, 70H99

Key words: Acoustics, high-frequency, Liouville equation, energy conservation, reflection, transmission.

1 Introduction

The present work deals with propagation of high-frequency acoustic waves at a straight interface between two homogeneous media characterized by their respective celerities and densities. The main issue that is considered here is the conservation of the total energy by the finite difference scheme used for numerical simulations. The overall propagation problem is splitted into two sub-problems, first propagation of high-frequency waves in both media itself, and second their behaviour at the interface considering reflection and transmission. Propagation is described by a Liouville transport equation which rules the evolution of the acoustic energy density in time and phase space (position $\times$ wave vector) [12]. It is solved numerically by a finite difference scheme [2, 9] applied in time and phase space following the original developments of Jin and co-workers [3–7]. The behaviour of the waves at the interface is described by Snell-Descartes laws [1, 8].

*Corresponding author. *Email addresses:* `joan.staudacher@ecp.fr` (J. Staudacher), `eric.savin@onera.fr` (É. Savin)

However the discontinuity of the celerities at that interface is a source of numerical dissipation, that is to say a net loss for the computed total acoustic energy. A refined interpolation of the acoustic energy density in the cells that have a common edge with the interface is necessary to obtain a conservative scheme. This interpolation has to be done on a wave-vector mesh which does not necessarily includes the reflected and/or transmitted wave vectors as given by Snell-Descartes laws. The main contribution of this paper is the derivation of an adapted finite difference scheme to circumvent this shortcoming. It is constructed in such a way that the (computed) overall acoustic energy remains conserved. The whole derivation is carried out for a two-dimensional acoustic medium, which is the plane of incidence of an acoustic source with a given incident wave vector. The diffraction phenomenon at critical incidence as considered by Jin and Yin [7] is however ignored in this work. It is the subject of ongoing research.

The physical model is recalled in Section 2, as well as the time and phase-space finite difference scheme introduced in [3–7]. The construction of a conservative scheme including reflection and transmission at the interface is outlined in Section 3. There the computation of the increment of the total acoustic energy between two successive time steps is performed and used as a guideline to construct explicitly an adapted interpolating expansion on the wave-vector grid. Both cases of transmission from the fast to the slow medium (Section 3.3), and from the slow to the fast medium (Section 3.4) are considered. Some comparisons of the proposed new scheme with the one of Jin and coworkers [3–7] are done through the numerical results given in Section 4. Finally Section 5 offers a few conclusions.

2 High-frequency acoustic wave propagation with a sharp interface

The transport model for high-frequency wave propagation in heterogeneous acoustic media derived in [12] is summarized in Section 2.1 below. It has been shown that the acoustic energy density associated to these waves satisfies a Liouville transport equation up to the interface. There it is reflected and/or transmitted according to Snell-Descartes laws [1] as recalled in Section 2.2. The last Subsection 2.3 describes how the Liouville equation is discretized by time and phase-space finite differences following an upwind scheme up to the interface.

2.1 Acoustic energy propagation

We consider the propagation of the high-frequency energy density in an acoustic medium $\mathcal{O} \subset \mathbb{R}^2$ divided into two subdomains $\mathcal{O}^-$ and $\mathcal{O}^+$ by a straight interface Γ oriented by its unit normal $\hat{\mathbf{n}}$. For convenience and without loss of generality this interface is the line $\Gamma = \{\mathbf{x} = (0,y),\ y \in \mathbb{R}\}$, thus $\mathcal{O}^- = \{\mathbf{x} = (x,y) \in \mathcal{O},\ x < 0\}$, $\mathcal{O}^+ = \{\mathbf{x} = (x,y) \in \mathcal{O},\ x > 0\}$ and we choose $\hat{\mathbf{n}} = (1,0)$. The tangent unit vector to the interface is denoted by $\hat{\mathbf{t}}$. The

sound speed $c(\mathbf{x})$ and the density $\varrho(\mathbf{x})$ are either the constants c^- and ϱ^- on the left side ($\mathbf{x}\in\mathcal{O}^-$) of Γ or the constants c^+ and ϱ^+ on its right side ($\mathbf{x}\in\mathcal{O}^+$). In the whole paper it is assumed that $c^-<c^+$. The acoustic wave equation in each subdomain for the pressure $p(t,\mathbf{x})$ is:

$$\frac{1}{c(\mathbf{x})^2}\partial_t^2 p-\Delta p=0, \tag{2.1}$$

with some initial conditions $p(0,\mathbf{x})=\epsilon A(\mathbf{x})e^{\mathrm{i}S(\mathbf{x})/\epsilon}$ and $\partial_t p(0,\mathbf{x})=B(\mathbf{x})e^{\mathrm{i}S(\mathbf{x})/\epsilon}$, where A and B denote amplitude functions depending on position $\mathbf{x}$ and S is for a phase function. ϵ is a small parameter which characterizes high frequencies. The initial conditions are supported in a compact subset of $\mathcal{O}^-$ or $\mathcal{O}^+$. In order to solve this system for $\epsilon\to 0$, we use the theory developed in [12] where it is shown that the energy density $a(t,\mathbf{x},\mathbf{k})$ of these high-frequency acoustic waves in the phase space $X=\mathcal{O}\times\mathbb{R}^2$ satisfies a Liouville transport equation:

$$\partial_t a+\nabla_{\mathbf{k}}\omega\cdot\nabla_{\mathbf{x}}a-\nabla_{\mathbf{x}}\omega\cdot\nabla_{\mathbf{k}}a=0, \tag{2.2}$$

where the Hamiltonian ω is $\omega(\mathbf{x},\mathbf{k})=c(\mathbf{x})|\mathbf{k}|$. Here $\mathbf{k}\in\mathbb{R}^2$ denotes the wave vector such that $\mathbf{k}=|\mathbf{k}|\hat{\mathbf{k}}$ and $\hat{\mathbf{k}}\in S^1$, the unit circle of $\mathbb{R}^2$. Thus the phase-space energy density a, also called specific intensity in the optical literature, is transported along rays which are the projections in physical space of the bicharacteristics of the Liouville equation (2.2). As in classical mechanics, the Hamiltonian ω is kept constant along a ray, even when it is being transmitted or reflected by an interface [1,11]. The overall energy $\mathcal{E}$ and power flow $\mathbf{\Pi}$ in the medium are recovered from the specific intensity by:

$$\mathcal{E}(t)=\int_X a(t,\mathbf{x},\mathbf{k})d\mathbf{x}d\mathbf{k},\qquad \mathbf{\Pi}(t)=\int_X a(t,\mathbf{x},\mathbf{k})\nabla_{\mathbf{k}}\omega d\mathbf{x}d\mathbf{k}.$$

We then focus on solving numerically the Liouville equation in X by finite differences following the scheme developed by Jin and co-workers in [3–7]. We seek a conservative scheme which works for rather coarse meshes of X, taking into account the reflection/transmission phenomena at the interface. The latter are described in the next Subsection 2.2. The scheme originally proposed in [3–7] is detailed in a subsequent subsection.

2.2 Acoustic waves reflection and transmission at an interface

At the interface Γ between two different media, an incident energy ray is partly transmitted and partly reflected, or totally reflected (above critical incidence). Let $\mathbf{k}_i$ be the wave vector of that incident ray, the wave vectors $\mathbf{k}_R$ and $\mathbf{k}_T$ of the reflected and transmitted rays, respectively, are such that the Hamiltonian is preserved:

$$\omega:=c^{\pm}|\mathbf{k}_i|=c^{\pm}|\mathbf{k}_R|=c^{\mp}|\mathbf{k}_T|. \tag{2.3}$$

For plane waves hitting the interface, this condition is equivalent to Snell-Descartes laws of refraction: the reflected and transmitted wave vectors $\mathbf{k}_R$ and $\mathbf{k}_T$ are located in the

plane of incidence $(\mathbf{k}_i,\hat{\mathbf{n}})$ and their tangential components are identical to the tangential component of the incident wave vector. Thus the following relations hold between their normal components $\xi_l=\mathbf{k}_l\cdot\hat{\mathbf{n}}$, $l=i,R$ or T:

$$\xi_r=-\xi_i,\qquad \xi_t=\text{sign}(\xi_i)\sqrt{\nu^2\xi_i^2+(\nu^2-1)\eta^2}, \tag{2.4}$$

where $\nu=c^-/c^+<1$ if $\xi_i>0$ (the incident wave impinges the interface from the left) or $\nu=c^+/c^->1$ if $\xi_i<0$ (the incident wave impinges the interface from the right). In the above $(\mathbb{I}-\hat{\mathbf{n}}\otimes\hat{\mathbf{n}})\mathbf{k}_l:=\eta\hat{\mathbf{t}}$ is the constant tangential component of the wave vectors, $\mathbb{I}$ being the identity matrix of $\mathbb{R}^2$. If $\nu<1$, ξ_t is purely imaginary above the critical incidence $\hat{\xi}_c:=\arccos\nu$, giving rise to evanescent surface waves. However the high-frequency energy density associated to the latter vanishes [1, 10, 11]. The associated acoustic power flow reflection/transmission coefficients are given by [1]:

$$\mathcal{R}^-(\omega,\eta)=\left(\frac{\varrho^+\xi_i-\varrho^-\xi_t}{\varrho^+\xi_i+\varrho^-\xi_t}\right)^2,\qquad \mathcal{T}^-(\omega,\eta)=1-\mathcal{R}^-(\omega,\eta),$$

for $\xi_i>0$; above critical incidence we set $\mathcal{R}^-(\omega,\eta)=1$ and thus $\mathcal{T}^-(\omega,\eta)=0$ (total reflection). The power flow reflection/transmission coefficients $\mathcal{R}^+(\omega,\eta)$ and $\mathcal{T}^+(\omega,\eta)$ for an incident ray hitting the interface from the right side $(\xi_i<0)$ are obtained from $\mathcal{R}^-(\omega,\eta)$ and $\mathcal{T}^-(\omega,\eta)$ by interchanging ϱ^+ and ϱ^-.

2.3 Finite-difference scheme in phase space

It is assumed in the remaining of the paper that the initial condition giving rise to high-frequency waves impinging the interface Γ is centered at a point $(\mathbf{x}_0,\mathbf{k}_0)$ of the phase space X, such that the wave vector $\mathbf{k}_0$ points toward the interface. The initial acoustic energy density is propagated according to (2.2) until it reaches Γ, where it is partially reflected and transmitted (diffraction at the critical incidence is ignored in our model).

The computational physical domain $\mathcal{O}_h=[-L_x,L_x]\times[-L_y,L_y]$ considered for numerical simulations is meshed uniformly by the grid points $\mathbf{x}_{i-\frac{1}{2},j-\frac{1}{2}}=(x_{i-\frac{1}{2}},y_{j-\frac{1}{2}})$ with $1\le i\le N_x+1$, $1\le j\le N_y+1$, such that $x_{i-\frac{1}{2}}=-L_x+(i-1)\Delta x$ and $y_{j-\frac{1}{2}}=-L_y+(j-1)\Delta y$, where $\Delta x=2L_x/N_x$ and $\Delta y=2L_y/N_y$. Then the mesh points $\mathbf{x}_{ij}=(x_i,y_j)$, $1\le i\le N_x$, $1\le j\le N_y$, at which the specific intensity a and the sound speed c are discretized, are defined by:

$$x_i=x_{i-\frac{1}{2}}+\frac{\Delta x}{2},\qquad y_j=y_{j-\frac{1}{2}}+\frac{\Delta y}{2}.$$

It is also assumed that there exists an index I such that $x_{I+\frac{1}{2}}=0$ is located on the interface; then I is the index of the cells adjacent to the left of the interface, and $I+1$ is the index of the cells adjacent to its right. A similar discretization is used for the wave vector $\mathbf{k}=(\xi,\eta)$, which is also taken in a bounded computational domain $[-K_x,K_x]\times[-K_y,K_y]$ $(K_x,K_y>0)$:

$$\xi_k=-K_x+\left(k-\frac{1}{2}\right)\Delta\xi,\qquad \eta_l=-K_y+\left(l-\frac{1}{2}\right)\Delta\eta,$$

for $1\leq k\leq N_\xi$ and $1\leq l\leq N_\eta$. $N_\xi=2K$ and N_η denote the number of mesh points and $\Delta\xi=2K_x/N_\xi$, $\Delta\eta=2K_y/N_\eta$. K is the index such that $\xi_k<0$ for $1\leq k\leq K$ and $\xi_k>0$ for $K+1\leq k\leq 2K$; this means that the case $\xi_k=0$ is excluded from our scheme, because, again, glancing energy rays are ignored. These rays shall be considered in future works, introducing a model of diffraction compatible with energetic quantities as considered here. The projection of the discretized wave vector $\mathbf{k}_{kl}=(\xi_k,\eta_l)$ on the unit circle is written $\hat{\mathbf{k}}_{kl}=(\hat{\xi}_{kl},\hat{\eta}_{kl})$, with:

$$\hat{\xi}_{kl}=\frac{\xi_k}{\sqrt{\xi_k^2+\eta_l^2}},\qquad \hat{\eta}_{kl}=\frac{\eta_l}{\sqrt{\xi_k^2+\eta_l^2}}.$$

At last, the discretized time steps are denoted by $t_n=n\Delta t$, $0\leq n\leq N$. It is assumed that N (for the last time step $\tau=N\Delta t$ of the computation) is such that the boundaries $x=\pm L_x$ and $y=\pm L_y$ of the computational physical domain $\mathcal{O}_h$ have not yet been reached, because we focus on the reflection/transmission processes on Γ solely. This assumption diverts us from dealing with any artificial or physical reflections on the boundaries, an issue out of the scope of the paper.

Then the fully discretized Liouville equation (2.2) is [3–7]:

$$\begin{aligned}&\frac{a^{n+1}_{ijkl}-a^n_{ijkl}}{\Delta t}+c_{ij}\hat{\xi}_{kl}\frac{a^n_{i+\frac12,jkl}-a^n_{i-\frac12,jkl}}{\Delta x}+c_{ij}\hat{\eta}_{kl}\frac{a^n_{i,j+\frac12,kl}-a^n_{i,j-\frac12,kl}}{\Delta y}\\&-\sqrt{\xi_k^2+\eta_l^2}\frac{c_{i+\frac12,j}-c_{i-\frac12,j}}{\Delta x}\frac{a^n_{ij,k+\frac12,l}-a^n_{ij,k-\frac12,l}}{\Delta\xi}-\sqrt{\xi_k^2+\eta_l^2}\frac{c_{i,j+\frac12}-c_{i,j-\frac12}}{\Delta y}\frac{a^n_{ijk,l+\frac12}-a^n_{ijk,l-\frac12}}{\Delta\eta}=0,\end{aligned}\quad(2.5)$$

with $c_{ij}=c(\mathbf{x}_{ij})$ for the sound speed on each cell. It requires to introduce for each mesh point (i,j,k,l) of the phase space and time step t_n four values $a^n_{i\pm\frac12,j\pm\frac12,kl}$ of the specific intensity computed from its values $a^n_{ijkl}\simeq a(t_n,\mathbf{x}_{ij},\mathbf{k}_{kl})$ by an upwind scheme. Given indices i, j, k, and l, the latter writes:

$$a^n_{i+\frac12,jkl}=a^n_{ijkl},\quad\text{if }\xi_k>0;\qquad a^n_{i+\frac12,jkl}=a^n_{i+1,jkl},\quad\text{if }\xi_k<0,\tag{2.6}$$

with similar expressions for $a^n_{i,j+\frac12,kl}$ along the y-axis as a function of the sign of η_l. The values $a^n_{i,j,k\pm\frac12,l\pm\frac12}$ for all cells are also given by an upwind scheme, which is described in [7] for example. Note that the fact that the sound speed is constant on each side of the interface implies that the fourth and fifth terms in Eq. (2.5) cancel. This full upwind scheme ensures the positivity of the solution for the cells that have no common edge with the interface. For the cells having an edge on the interface, the reflection and transmission processes must be taken into account in the definition of the numerical fluxes. The extension of the upwind scheme in these cells is based on the conservation of the discretized normal flux densities $c_{ij}\hat{\xi}_{kl}a^n_{ijkl}$ at the interface, which is written:

$$c^-\hat{\xi}_{kl}a^n_{I+\frac12,jkl}=c^-R^-(k_R,l)\hat{\xi}_{kl}a^n_{I,jk_Rl}+c^+T^+(k_T,l)\hat{\xi}_{k_Tl}a^n_{I+1,jk_Tl},\qquad\text{if }\xi_k<0,\tag{2.7a}$$

$$c^+\hat{\xi}_{kl}a^n_{I+1-\frac12,jkl}=c^+R^+(k_R,l)\hat{\xi}_{kl}a^n_{I+1,jk_Rl}+c^-T^-(k_T,l)\hat{\xi}_{k_Tl}a^n_{I,jk_Tl},\qquad\text{if }\xi_k>0,\tag{2.7b}$$

where:

$$R^{\pm}(k,l) := \mathcal{R}^{\pm}\Big(c^{\pm}\sqrt{\xi_k^2+\eta_l^2},\eta_l\Big), \qquad T^{\pm}(k,l) := \mathcal{T}^{\pm}\Big(c^{\pm}\sqrt{\xi_k^2+\eta_l^2},\eta_l\Big),$$

using the power flow reflection/transmission coefficients $\mathcal{R}^{\pm}(\omega,\eta)$ and $\mathcal{T}^{\pm}(\omega,\eta)$ introduced in Section 2.2. In the above $a^n_{Ijk_Rl}$, a^n_{I+1,jk_Rl}, $a^n_{Ijk_Tl}$ and a^n_{I+1,jk_Tl} are the discretized specific intensities corresponding to some incident wave vectors $\mathbf{k}_{k_Rl}=(\xi_R,\eta_l)$ and $\mathbf{k}_{k_Tl}=(\xi_T,\eta_l)$, yielding the wave vector $\mathbf{k}_{kl}=(\xi_k,\eta_l)$ by reflection and transmission respectively. By symmetry ξ_R is directly obtained from ξ_k by $\xi_R=-\xi_k$ (or $k_R=2K+1-k$ from the definition of the discretized phase space). However, ξ_T is not necessarily a mesh point and k_T does not necessarily correspond to an index on this mesh. In [3–7], $a^n_{ijk_Tl}$ for $i=I$ or $i=I+1$ is written as a linear interpolation of $a^n_{ijk'l}$ and $a^n_{ij,k'+1,l}$ for the index k' such that $\xi_{k'}<\xi_T<\xi_{k'+1}$. But this scheme has no reason to be conservative *a priori*. The purpose of the paper is to present a refined interpolation by enforcing conservation of the discretized total energy. It is described in the next section.

3 Conservative finite differences scheme

Dividing the previous equalities (2.7) by $c^-\hat{\xi}_{kl}$ and $c^+\hat{\xi}_{kl}$, respectively, the discretized specific intensities on the interface are written in the form:

$$a^n_{I+\frac{1}{2},jkl} = R^-(k_R,l)b^n_{Ijk_Rl} + T^+(k_T,l)b^n_{I+1,jk_Tl}, \qquad \text{if } \xi_k<0, \tag{3.1a}$$

$$a^n_{I+1-\frac{1}{2},jkl} = R^+(k_R,l)b^n_{I+1,jk_Rl} + T^-(k_T,l)b^n_{Ijk_Tl}, \qquad \text{if } \xi_k>0, \tag{3.1b}$$

where $b^n_{ijk_Rl}$ and $b^n_{ijk_Tl}$ are defined so as to conserve the discretized total energy for all time steps of the simulation. Their construction is the main ingredient of the proposed new numerical scheme. It is summarized in the following Section 3.1, whereas the increment of the discretized total energies for two successive time steps is computed in Section 3.2. Equating it to zero yields the required interpolation coefficients introduced in Section 3.1; this is done for an incident wave impinging the interface from the right (fast to slow medium) in Section 3.3 or from the left (slow to fast medium) in Section 3.4.

Now let us define some notations used in the remaining of the paper. As η_l is a constant parameter all along the reflection/transmission process, it is simply noted η in the following in order to lighten notations, for it is understood that it should be fixed among the mesh points $\{\eta_l\}_{1\le l\le N_\eta}$. Second, for some normal wave-vector component ξ within the computational wave-vector domain, we will use the mapping $\xi\mapsto \mathsf{index}(\xi)$ which identifies the index k of the closest mesh point ξ_k to ξ; it is defined by:

$$\mathsf{index}(\xi) := \Big[\frac{\xi+K_x}{\Delta\xi}+\frac{1}{2}\Big],$$

where $[z]$ stands for the integer part of $z\in\mathbb{R}$.

3.1 Discretized specific intensities at the interface

The expressions for $b^n_{ijk_Rl}$ and $b^n_{ijk_Tl}$, with $i=I$ or $i=I+1$ are specific to the scheme used to ensure the conservation of the discretized normal fluxes on the interface. First, in the case of a straight interface, the symmetry of the mesh points $\{\xi_k\}_{1\le k\le 2K}$ yields:

$$b^n_{ijk_Rl}=a^n_{ij,2K+1-k,l}.$$

Second, the transmitted specific intensity $b^n_{ijk_Tl}$ for $i=I$ or $I+1$ is written as a linear combination of the discretized specific intensities a^n_{ijkl} of the form:

$$b^n_{ijk_Tl}=\sum_{p=k'-K_m}^{k'+K_M}\gamma_p a^n_{ijpl}, \tag{3.2}$$

where the scalars γ_p and the strictly positive integers K_m and K_M are chosen by enforcing conservation of the discretized total energy computed in the next section. The index k' is $k'=\mathrm{index}(\xi_T)$, where ξ_T is derived from Eq. (2.4) by $\xi_k=(\nu^2\xi_T^2+(\nu^2-1)\eta^2)^{1/2}$. Again, ξ_T as given by the latter formula has no reason to be a mesh point, hence the interpolation (3.2).

3.2 Evolution of the discretized total energy

The discretized total energy $\mathcal{E}^n_a$ of the medium at time t_n is given by the discrete ℓ^1-norm of a^n in phase space:

$$\mathcal{E}^n_a=\Delta x\Delta y\Delta\xi\Delta\eta\sum_{ijkl}a^n_{ijkl}:=\|a^n\|_1.$$

Using the discretized Liouville equation (2.5) and the upwind fluxes, yields the following equality for $\mathcal{E}^{n+1}_a$ and $\mathcal{E}^n_a$:

$$\mathcal{E}^n_a-\mathcal{E}^{n+1}_a=\Delta t\Delta\xi\Delta\eta\Big(\Delta y\sum_{ij}c_{ij}\sum_{kl}\hat{\xi}_{kl}\big(a^n_{i+\frac{1}{2},j,kl}-a^n_{i-\frac{1}{2},j,kl}\big)+\Delta x\sum_{ij}c_{ij}\sum_{kl}\hat{\eta}_{kl}\big(a^n_{i,j+\frac{1}{2},kl}-a^n_{i,j-\frac{1}{2},kl}\big)\Big).$$

For all indices i, k, l, and n let:

$$S^n_{ikl}=\frac{\Delta t}{\Delta y}\hat{\eta}_{kl}\sum_{j=1}^{N_y}c_i\big(a^n_{i,j+\frac{1}{2},kl}-a^n_{i,j-\frac{1}{2},kl}\big),$$

where $c_i=c^-$, if $i\le I$ and $c_i=c^+$, if $i\ge I+1$, as the interface is vertical. Since an upwind scheme is used, we have:

$$S^n_{ikl}=\begin{cases}\dfrac{\Delta t}{\Delta y}\hat{\eta}_{kl}\displaystyle\sum_{j=1}^{N_y}c_i(a^n_{ijkl}-a^n_{i,j-1,kl})=\dfrac{\Delta t}{\Delta y}\hat{\eta}_{kl}c_i(a^n_{i,N_y,kl}-a^n_{i0kl}), & \text{if } \eta>0,\\[2ex] \dfrac{\Delta t}{\Delta y}\hat{\eta}_{kl}\displaystyle\sum_{j=1}^{N_y}c_i(a^n_{i,j+1,kl}-a^n_{ijkl})=\dfrac{\Delta t}{\Delta y}\hat{\eta}_{kl}c_i(a^n_{i,N_y+1,kl}-a^n_{i1kl}), & \text{if } \eta<0.\end{cases}$$

For all time steps we have assumed above that

$$a^n_{iN_ykl}=a^n_{i0kl}=0 \quad \text{and} \quad a^n_{i,N_y+1,kl}=a^n_{i1kl}=0$$

for all indices i, k and l, because the boundaries of the computational physical domain $\mathcal{O}_h$ are never reached during the simulation; in addition the values of the specific intensities outside $\mathcal{O}_h$ namely $a^n_{i,N_y+1,kl}$ and a^n_{i0kl}, are conventionally set to zero. Under these assumptions, each of the sums S^n_{ikl} is zero and the total sum $\sum_{k,l} S^n_{ikl}$ is also equal to zero. Likewise for all indices j, k, l, we set

$$a^n_{N_x,jkl}=a^n_{0,jkl}=0 \quad \text{and} \quad a^n_{N_x+1,jkl}=a^n_{1,jkl}=0,$$

such that the following sum S rewrites:

$$S:=\frac{\Delta t}{\Delta x}\sum_{ij}c_i\sum_{kl}\hat{\xi}_{kl}\left(a^n_{i+\frac{1}{2},jkl}-a^n_{i-\frac{1}{2},jkl}\right)=\frac{\Delta t}{\Delta x}\sum_{j}\left(\sum_{kl}c^-\hat{\xi}_{kl}a^n_{I+\frac{1}{2},jkl}-\sum_{kl}c^+\hat{\xi}_{kl}a^n_{I+1-\frac{1}{2},jkl}\right).$$

We then deduce that the difference $\mathcal{E}^n_a-\mathcal{E}^{n+1}_a=S\times\Delta x\Delta y\Delta\xi\Delta\eta$ is a function of the discretized specific intensities at the interface, as expected. The latter are $a^n_{I+\frac{1}{2},jkl}$ and $a^n_{I+1-\frac{1}{2},jkl}$ as defined in Eq. (3.1), and they must be chosen to ensure the conservation of the discretized total energy between two time steps. Let us rewrite:

$$S=\frac{\Delta t}{\Delta x}\sum_{jl}\left[\sum_{k;\xi_k>0}\left(c^-\hat{\xi}_{kl}a^n_{I+\frac{1}{2},jkl}-c^+\hat{\xi}_{kl}a^n_{I+1-\frac{1}{2},jkl}\right)+\sum_{k;\xi_k<0}\left(c^-\hat{\xi}_{kl}a^n_{I+\frac{1}{2},jkl}-c^+\hat{\xi}_{kl}a^n_{I+1-\frac{1}{2},jkl}\right)\right],$$

then taking into account that by upwinding, Eq. (2.6),

$$a^n_{I+\frac{1}{2},jkl}=a^n_{Ijkl}, \quad \text{if } \xi_k>0; \qquad a^n_{I+1-\frac{1}{2},jkl}=a^n_{I+1,jkl}, \quad \text{if } \xi_k<0,$$

invoking again Eq. (3.1), and then using a change of variables for the reflected vectors, the expression of S is finally merged to $S=S_1+S_2$ where:

$$S_1=\frac{\Delta t}{\Delta x}\sum_{jl}\sum_{k=1}^{K}\left(c^-T^+(k_T,l)\hat{\xi}_{kl}b^n_{I+1,jk_Tl}-c^+(1-R^+(k,l))\hat{\xi}_{kl}a^n_{I+1,jkl}\right),$$

$$S_2=\frac{\Delta t}{\Delta x}\sum_{jl}\sum_{k=K+1}^{2K}\left(c^-(1-R^-(k,l))\hat{\xi}_{kl}a^n_{Ijkl}-c^+T^-(k_T,l)\hat{\xi}_{kl}b^n_{Ijk_Tl}\right).$$

Cancelling S as expressed above yields $\mathcal{E}^{n+1}_a=\mathcal{E}^n_a$ or $\|a^{n+1}\|_1=\|a^n\|_1$, which is the conservative property, or ℓ^1-stability sought for. The next Sections 3.3 and 3.4 describe how to choose the expansion (3.2) of $b^n_{Ijk_Tl}$ and b^n_{I+1,jk_Tl} in order to satisfy this property. It should be noted that the numerical fluxes constructed by this process are first order in $\mathbf{x}$ and $\mathbf{k}$, but this order could actually be increased using a slope limiter as in [6] for example. The algorithm described there enables to obtain a second order accuracy and could be extended to our scheme; we will not however pursue this issue in the remaining of the paper but shall rather leave it to future works.

3.3 Transmission from the fast to the slow medium

Let us first consider the case when the initial energy density is on the right side of the interface and propagates toward it. Let n be a time index for which none of the physical boundaries has yet been reached. Then the values of a^n_{Ijkl} for $\xi_k>0$ and thus the values of $b^n_{Ijk_Tl}$ vanish, as well as the values $a^n_{Ijk_Rl}$ for $\xi_k>0$, since no wave impinges the interface from the left. Thus $S_2=0$ and S reduces to S_1. To obtain a conservative scheme, we have to choose b^n_{I+1,jk_Tl} such that $S_1=0$.

Let k be a given index such that $\xi_k<0$, and η (the constant discretized tangent wave vector) is a fixed real parameter among the mesh points $\{\eta_l\}_{1\le l\le N_\eta}$. The incident energy density on the fast side with wave vector (ξ_T,η) is transmitted by the interface in the direction defined by the wave vector (ξ_k,η). Then b^n_{I+1,jk_Tl} is approximated using the existing mesh of wave vectors and Eq. (3.2). To determine the relationship between the incident wave vector and a given transmitted wave vector from the mesh $\{\mathbf{k}_{kl}\}$, let us consider the function $f_\eta:[-\infty,\Xi_\eta]\to[-\infty,0]$ defined by:

$$f_\eta(\xi)=-\frac{1}{\nu}\sqrt{\xi^2+(1-\nu^2)\eta^2},$$

where $\Xi_\eta=-|\eta|\sqrt{\nu^2-1}$ such that $f_\eta(\Xi_\eta)=0$ and $\{(\xi,\eta);\xi<\Xi_\eta\}$ is included in the set of sub-critical vectors. It is reminded that in this configuration $\nu=c^+/c^->1$. Also f_η is an increasing continuous function, and it has an asymptotic direction given by $\xi\mapsto\xi/\nu$ for $\xi\to-\infty$ (see Fig. 1). Then as $\nu>1$, there is a unique normal wave-vector component $\Xi'_\eta=-\nu|\eta|$ such that

$$f'_\eta(\Xi'_\eta)=1 \quad\text{and}\quad f'_\eta(\xi)<1, \qquad \text{for all } \xi<\Xi'_\eta.$$

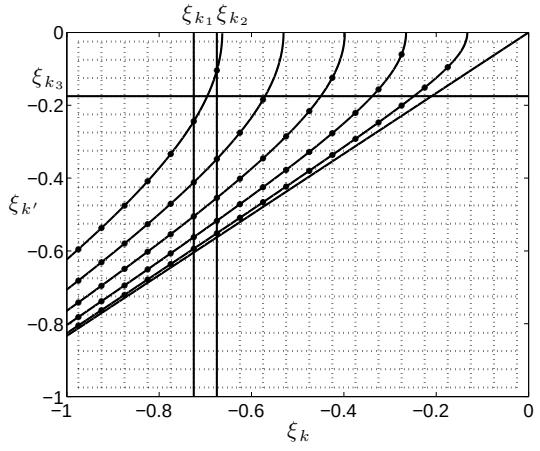

Figure 1: The function $f_\eta:\xi\mapsto-\frac{1}{\nu}\sqrt{\xi^2+(1-\nu^2)\eta^2}$ with $\eta=0.2$, $\eta=0.4$, $\eta=0.6$, $\eta=0.8$ and 1.0 from the right to the left, and $\nu=c^+/c^-=1.2$; wave-vector normal component mesh for $K=20$ (dotted lines $\cdots$) and its intersections with f_η (bullets $\bullet$).

Let us define the indices $k_\eta = \mathsf{index}(\Xi_\eta)$ and $k'_\eta = \mathsf{index}(\Xi'_\eta) \le k_\eta$ of the wave vector meshes for the closest grid points to Ξ_η and Ξ'_η, and introduce the sets $\mathcal{K}_k$ and $\mathcal{J}_{\eta,k}$ defined for $1 \le k \le k_\eta$ by

$$\mathcal{K}_k = \{\xi_1, \xi_2, \cdots, \xi_k\}, \qquad \mathcal{J}_{\eta,k} = \{k';\, k' = \mathsf{index}(f_\eta(\xi)), \xi \in \mathcal{K}_k\},$$

and denote $\mathcal{J}_\eta = \mathcal{J}_{\eta,k_\eta}$. As f_η is a monotonous function, one can always find an index $k' \in \mathcal{J}_{\eta,k}$ such that $\xi_{k'} \le f_\eta(\xi_k) < \xi_{k'+1}$; then a two-point interpolation for b^n_{I+1,jk_Tl} may be chosen in the form:

$$b^n_{I+1,jk_Tl} = \gamma_1(k',l) a^n_{I+1,jk'l} + \gamma_2(k'+1,l) a^n_{I+1,j,k'+1,l}, \tag{3.3}$$

where $k' = \mathsf{index}(f_\eta(\xi_k))$. However, the set $\mathcal{J}^{+1}_\eta := \mathcal{J}_\eta \cup \{\mathcal{J}_\eta + 1\}$ does not contain all the indices $\{1,2,\cdots,K\}$, and some points of the wave-vector mesh may never be covered by such a two-point interpolation. In fact, as soon as $k \le k'_\eta$ the set $\mathcal{J}^{+1}_{\eta,k} := \mathcal{J}_{\eta,k} \cup \{\mathcal{J}_{\eta,k} + 1\}$ has a sequential form

$$\mathcal{J}^{+1}_{\eta,k} = \{k_m, k_m+1, \cdots, k_M-1, k_M\},$$

where $k_m \ge 1$ and $k_M \le K$. But for $k > k'_\eta$ this is not necessarily the case. This situation is illustrated for example on Fig. 1 below for the grid point ξ_{k_3} corresponding to the horizontal thick line: this point is never covered by the two-point interpolations (3.3) constructed from ξ_{k_1} and ξ_{k_2}. This means that the set $\mathcal{J}^{+1}_{\eta,k_2}$ is not sequential, and more points need be used in this case for the interpolation. This occurrence is described more in detail in the following Section 3.4. Nevertheless, for the ease of understanding, we assume in the remaining of this section that the above two-point interpolation is sufficient for all cases. This means that for the largest index $k > k'_\eta$ such that the set $\mathcal{J}^{+1}_{\eta,k}$ is sequential, the upper bound k_M is equal to K (note that this assumption will be released in the next section). Then plugging (3.3) in S_1 yields:

$$\begin{aligned}
\frac{\Delta x}{\Delta t} S_1 = \sum_{jl} \Bigg[& \sum_{k=1}^{k_\eta} c^- T^+(k_T,l) \hat{\xi}_{kl} \Big(\gamma_1(k',l) a^n_{I+1,jk'l} + \gamma_2(k'+1,l) a^n_{I+1,j,k'+1,l} \Big) \\
& - \sum_{k=1}^{K} c^+ (1 - R^+(k,l)) \hat{\xi}_{kl} a^n_{I+1,jkl} \Bigg] \\
= \sum_{jl} c^- \Bigg[& \sum_{k' \in \mathcal{J}_\eta} \Big(\sum_{k;\, \xi_{k'} < f_{\eta_l}(\xi_k) < \xi_{k'+1}} T^+(k_T,l) \hat{\xi}_{kl} \Big) \gamma_1(k',l) a^n_{I+1,jk'l} \\
& + \sum_{k' \in \mathcal{J}_\eta + 1} \Big(\sum_{k;\, \xi_{k'-1} < f_{\eta_l}(\xi_k) < \xi_{k'}} T^+(k_T,l) \hat{\xi}_{kl} \Big) \gamma_2(k',l) a^n_{I+1,j,k'l} \Bigg] \\
& - \sum_{jl} \sum_{k'=1}^{K} c^+ (1 - R^+(k',l)) \hat{\xi}_{k'l} a^n_{I+1,jk'l}.
\end{aligned}$$

For $\eta = \eta_l$ fixed (l fixed), the lower bound of $\mathcal{J}^{+1}_\eta$ is $k_m = \mathsf{index}(f_\eta(\xi_1))$. Then it is finally assumed that $a^n_{I+1,jk'l} = 0$ for all $k' < k_m$, so that only the part of the wave vectors $(\xi_{k'}, \eta)$

with $k' \geq k_m$ can be transmitted. Note that this assumption is naturally imposed by the boundedness of the computational wave-vector domain $[-K_x,K_x]\times[-K_y,K_y]$. By merging the sums above, expressions for the coefficients γ_1 and γ_2 are finally obtained as:

$$\gamma_1(k',l) = \frac{\nu(1-R^+(k',l))\hat{\xi}_{k'l}}{2\sum_{k;\ \xi_{k'}<f_\eta(\xi_k)<\xi_{k'+1}} T^+(k_T,l)\hat{\xi}_{kl}}, \qquad \forall k' \in \mathcal{J}_\eta, \tag{3.4a}$$

$$\gamma_2(k',l) = \frac{\nu(1-R^+(k',l))\hat{\xi}_{k'l}}{2\sum_{k;\ \xi_{k'-1}<f_\eta(\xi_k)<\xi_{k'}} T^+(k_T,l)\hat{\xi}_{kl}}, \qquad \forall k' \in \mathcal{J}_\eta+1. \tag{3.4b}$$

Using them in Eq. (3.3) allows to derive a conservative scheme for the energy rays crossing the interface from the fast to the slow medium as illustrated on Fig. 4 below. The proposed scheme also inherits the positivity property of the original scheme in [3–7] with a similar hyperbolic-type CFL condition. Finally, the above coefficients can be majorized independently of k' such that one obtains $|b^n_{I+1,jk_Tl}| \leq C\|a^n\|_\infty$ for some constant $C>0$ and this scheme is ℓ^∞-stable as well.

3.4 Transmission from the slow to the fast medium

Let us now consider the case when the initial energy density is on the left side of the interface and propagates toward it. n is again a time step for which none of the physical boundaries has been reached yet. As before, the values of $a^n_{I+1,jkl}$ with $\xi_k<0$ and thus the values of b^n_{I+1,jk_Tl} vanish, as well as the values a^n_{I+1,jk_Rl} with $\xi_k<0$, since no wave impinges the interface from the right. Thus $S_1=0$ and S reduces to S_2. To obtain a conservative scheme, we have to choose $b^n_{Ijk_Tl}$ such that $S_2=0$.

Let k a given index such that $\xi_k>0$, and η be again a fixed real parameter among the mesh points $\{\eta_l\}_{1\leq l\leq N_\eta}$. As in Section 3.3, the incident specific intensity on the slow side with wave vector (ξ_T,η) is transmitted by the interface in the direction defined by the wave vector (ξ_k,η). Then $b^n_{Ijk_Tl}$ is approximated using the existing mesh of wave vectors and Eq. (3.2). To determine the relationship between the incident wave vector and a given transmitted wave vector from the mesh $\{\mathbf{k}_{kl}\}$, we consider now the function $g_\eta:[0,+\infty]\to[\overline{\Xi}_\eta,+\infty]$ defined by:

$$g_\eta(\xi) = \frac{1}{\nu}\sqrt{\xi^2+(1-\nu^2)\eta^2},$$

where $\overline{\Xi}_\eta = \eta\sqrt{1-\nu^2}/\nu = -\Xi_\eta$ has been defined in the previous section as the normal wave-vector component corresponding to the critical angle. The analysis of g_η shows that it is an increasing function, that it has an asymptotic direction $\xi\mapsto\xi/\nu$ for $\xi\to+\infty$, but contrary to the previous case its slope is $1/\nu=c^+/c^->1$ in this configuration (see Fig. 2). Also the normal component Ξ''_η such that $g'_\eta(\Xi''_\eta)=1$ is $\Xi''_\eta=\nu\eta$, corresponding to the index $k''_\eta=\mathsf{index}(\Xi''_\eta)$ of the mesh.

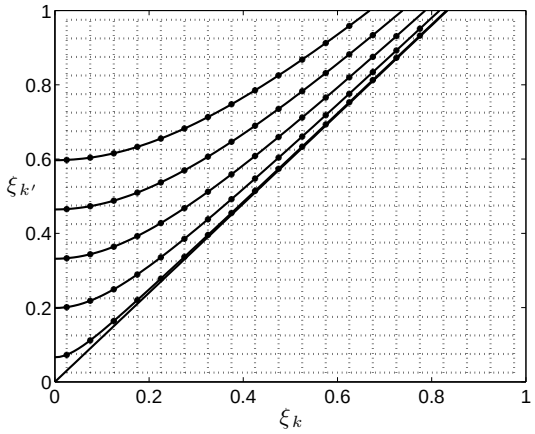

Figure 2: The function $g_\eta : \xi \mapsto \frac{1}{\nu}\sqrt{\xi^2+(1-\nu^2)\eta^2}$ with $\eta=0.1$, $\eta=0.3$, $\eta=0.5$, $\eta=0.7$, and $\eta=0.9$ from the bottom to the top, and $1/\nu = c^+/c^- = 1.2$; wave-vector normal component mesh for $K=20$ (dotted lines $\cdots$) and its intersections with g_η (bullets $\bullet$).

Now let us introduce the normal component Ξ_d such that $g(\Xi_d)=\xi_{2K}$ and the sets $\mathcal{K}_k$ and $\mathcal{J}_{\eta,k}$ now defined for $K+1\le k\le k_d = \mathsf{index}(\Xi_d)$ by

$$\mathcal{K}_k = \{\xi_k, \xi_{k+1}, \cdots, \Xi_d\}, \qquad \mathcal{J}_{\eta,k} = \{k';\ k' = \mathsf{index}(g_\eta(\xi)),\ \xi \in \mathcal{K}_k\}.$$

Assuming that $\xi_{k''_\eta+1} < \Xi_d$, then $g'_\eta(\xi_k) < 1$ for $K+1 \le k \le k''_\eta$, and the two-point interpolation (3.3) can be used in this case:

$$b^n_{Ijk_T l} = \gamma_1(k',l)\, a^n_{Ijk'l} + \gamma_2(k'+1,l)\, a^n_{Ij,k'+1,l}, \tag{3.5}$$

where $k' = \mathsf{index}(g_\eta(\xi_k))$. As already outlined in Section 3.4, it is however not sufficient if the set $\mathcal{J}^{+1}_{\eta,K+1} = \mathcal{J}_{\eta,K+1} \cup \{\mathcal{J}_{\eta,K+1}+1\}$ is different from the sequential set $\{2K-k_\eta, 2K-k_\eta+1, \cdots, 2K-1, 2K\}$, where one can check that $2K-k_\eta = \mathsf{index}(-\Xi_\eta)$ and k_η has been introduced above in Section 3.3. That is to say that the previous set does not cover all the mesh points in the computational wave-vector domain and thus contains holes. Indeed, as the slope of g_η may be greater than 1, it may happen that some mesh points can not be counted in the set $\mathcal{J}^{+1}_{\eta,K+1}$; then (3.5) misses all the a^n_{Ijkl}'s for the k's not included in it. Thus for $k''_\eta+1 \le k \le k_d$ the interpolation is defined by:

$$b^n_{Ijk_T l} = \sum_{p\in\mathcal{I}(k)} \gamma_k(p,l)\, a^n_{Ijpl}, \tag{3.6}$$

where the sets $\mathcal{I}(k)$ are defined such that $\mathsf{index}(g_\eta(\xi_k)) \in \mathcal{I}(k)$, $\mathcal{I}(k_1) \cap \mathcal{I}(k_2) = \varnothing$, for $k_1 \neq k_2$, and

$$\bigcup_k \mathcal{I}(k) = \{2K-k_\eta, 2K-k_\eta+1, \cdots, 2K\}.$$

Also because of the boundedness of the computational wave-vector domain it can be assumed that $a^n_{Ijk'l}=0$ for all $k'>k_d$.

Then plugging Eq. (3.6) in S_2, the latter rewrites:

$$\begin{aligned}\frac{\Delta x}{\Delta t}S_2=\sum_{jl}\Bigg[&\sum_{k=K+1}^{2K-k_\eta}c^-(1-R^-(k,l))\hat{\xi}_{kl}a^n_{Ijkl}-\sum_{k=K+1}^{k''_\eta}c^+T^-(k_T,l)\hat{\xi}_{kl}b^n_{Ijk_Tk}\\&-\sum_{k=2K-k_\eta+1}^{\min(\mathcal{I}(k''_\eta+1))-1}c^-(1-R^-(k,l))\hat{\xi}_{kl}a^n_{Ijkl}\\&-\sum_{k=k''_\eta+1}^{k_d}\sum_{p\in\mathcal{I}(k)}\Big(c^+T^-(k_T,l)\gamma_k(p,l)\hat{\xi}_{kl}a^n_{Ijpl}-c^-(1-R^-(p,l))\hat{\xi}_{pl}a^n_{Ijpl}\Big)\Bigg].\end{aligned}$$

The first sum in the above expression cancels because it corresponds to total reflection with $R^-(k,l)=1$. The second and third sums are cancelled with the regular two-point interpolation of Eq. (3.5). At last the interpolation coefficients $\gamma_k(p,l)$ are chosen such that the fourth sum cancels for all $p\in\mathcal{I}(k)$, that is:

$$\gamma_k(p,l)=\frac{\nu(1-R^-(p,l))\hat{\xi}_{pl}}{T^-(k_T,l)\hat{\xi}_{kl}},\qquad\forall p\in\mathcal{I}(k).\tag{3.7}$$

These coefficients as well as γ_1 and γ_2 in (3.5) may be majorized independently of p or k', yielding $|b^n_{Ijk_Tl}|\le C\|a^n\|_\infty$, for some constant $C>0$ and thus the ℓ^∞-stability of the proposed scheme, as in Section 3.3.

4 Numerical results

In this section we present some numerical results obtained with the proposed conservative scheme and compare them with those obtained with the scheme depicted in [3–7]. In the latter the b_{ijkl}'s of Eq. (3.1) are constructed by linear interpolation:

$$b^n_{ijk_Tl}=\frac{\xi_{k'+1}-\xi_T}{\Delta\xi}a^n_{ijk'l}+\frac{\xi_T-\xi_{k'}}{\Delta\xi}a^n_{ij,k'+1,l},\quad b^n_{ijk_Rl}=\frac{\xi_{k_1+1}-\xi_R}{\Delta\xi}a^n_{ijk_1l}+\frac{\xi_R-\xi_{k_1}}{\Delta\xi}a^n_{ij,k_1+1,l},\tag{4.1}$$

for $i=I$ or $I+1$, with $k'=\mathsf{index}(\xi_T)$, $k_1=N_\xi+1-k$, $\xi_R=-\xi_k$, and $\xi_T=f_\eta(\xi_k)$, if $\xi_k<0$ or $\xi_T=g_\eta(\xi_k)$, if $\xi_k>0$. The sound speeds on both sides of the interface are $c^-=1$ and $c^+=2.5$ for both computations presented below, and we consider a computational physical domain with $L_x=0.4$ and $L_y=0.25$. The first computation is for reflection/transmission of the specific intensity from the fast to the slow medium. The phase-space mesh is constructed with the following data: $N_x=N_y=N_\eta=36$, and $K=25$; the Courant number for time discretization is $C:=c^-\Delta t/\Delta x=1/14$. The initial specific intensity $a^0_{ijkl}=a^0(\mathbf{x}_{ij},\mathbf{k}_{kl})$ is given by:

$$a^0(\mathbf{x},\mathbf{k})=\frac{1}{\pi c_1^2}e^{-\left(\frac{|\mathbf{x}-\mathbf{x}_0|}{c_2}\right)^2}\times e^{-\left(\frac{|\mathbf{k}-\mathbf{k}_0|}{c_1}\right)^2}\times\varphi_{2\Delta\mathbf{x}}(\mathbf{x}-\mathbf{x}_0)\times\varphi_{2\Delta\mathbf{k}}(\mathbf{k}-\mathbf{k}_0),\tag{4.2}$$

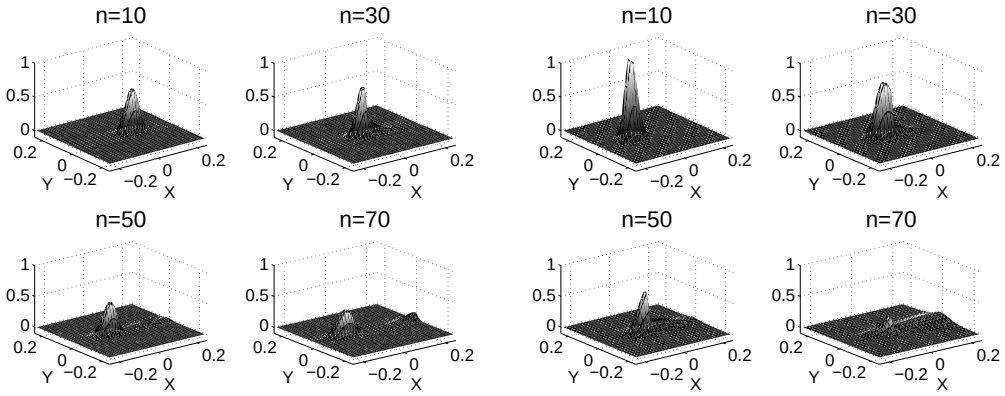

Figure 3: Snapshots of the specific intensities computed by the proposed new scheme at time steps $t_n = 10\times\Delta t$, $t_n = 30\times\Delta t$, $t_n = 50\times\Delta t$, and $t_n = 70\times\Delta t$ with $c^- = 1$, $c^+ = 2.5$, and Courant number $C = 1/14$; propagation from the fast to the slow medium (left) and from the slow to the fast medium (right).

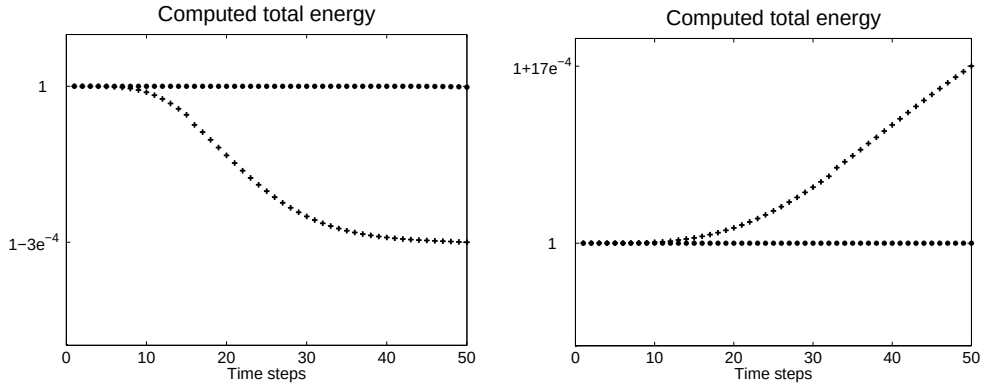

Figure 4: Evolution of the computed total energy for the proposed new scheme (•) and for the scheme of [7] (+); propagation from the fast to the slow medium (left) and from the slow to the fast medium (right).

where $c_1 = 0.02$, $c_2 = 0.025$, $\mathbf{x}_0 = (0.1083,0)$, $\mathbf{k}_0 = (-0.09,0)$; and $\varphi_{\Delta\mathbf{x}}(\mathbf{x})$ is the characteristic function

$$\varphi_{\Delta\mathbf{x}}(\mathbf{x}) = \mathbf{1}_{\{|x|\le\Delta x\}}(x)\times\mathbf{1}_{\{|y|\le\Delta y\}}(y)$$

with a similar definition for $\varphi_{\Delta\mathbf{k}}(\mathbf{k})$. The initially peaked specific intensity a^0 is a truncated Gaussian beam centered around the point $(\mathbf{x}_0,\mathbf{k}_0)$ in phase space which propagates toward the interface Γ. Although it is discontinuous, the proposed scheme is observed to be numerically convergent in agreement with [4, 5] for one-dimensional examples. A second computation considers propagation from the slow to the fast medium. In this case the phase-space mesh is constructed with the following data: $N_x = N_y = N_\eta = 30$ and $K = 20$, while the Courant number is the same as in the previous example. The initial specific intensity is (4.2) with $\mathbf{x}_0 = (-0.1083,0)$ and $\mathbf{k}_0 = (0.17,0)$. Fig. 3 displays some snapshots of the computed specific intensity at different time steps for both computations. Fig. 4 also

displays the evolution of the total acoustic energy during the simulation, as computed by the proposed modified scheme (labelled with bullets •) and by the original scheme of [7] with reflected and transmitted specific intensities given by Eq. (4.1) (labelled with pluses $+$).

5 Conclusions and perspectives

In this paper, we have modified the numerical scheme proposed in [3–7] to solve the Liouville equation for the high-frequency acoustic energy density in a two dimensional domain divided into two sub-domains with different sound speeds by a straight interface. The proposed new scheme is a phase-space finite difference scheme which takes into account (i) the reflection/transmission phenomena, and (ii) conserves the total acoustic energy reflected and transmitted by the interface. The evolution of the total energy between two successive time steps is computed, and an interpolation formula for the computed energy density is derived on each side of the interface. More precisely, interpolation weights on the wave-vector grid are derived for transmission from the fast to the slow medium (see Eq. (3.4)) as well as transmission from the slow to the fast medium (see Eq. (3.7)). At present the proposed scheme is limited to a straight interface and a piecewise homogeneous medium. A scheme for a curved interface in two dimensions will be derived along the same way in future works. Its possible extension to heterogeneous acoustic media (at least away from the interface), as implemented in [4–6], shall be investigated as well. Diffraction phenomena have been considered in [7], but not in this paper. They shall also be taken into account in future researches. We note finally that the ideas presented in this paper may be extended in our opinion to higher-order schemes, using slope limiters for example [6], and adaptive strategies.

References

[1] G. Bal, J. B. Keller, G. C. Papanicolaou and L. V. Ryzhik, Transport theory for acoustic waves with reflection and transmission at interfaces, Wave Motion, 30 (1999), 303–327.
[2] Gary C. Cohen, Higher-Order Numerical Methods for Transient Wave Equations, Springer, 2002.
[3] S. Jin and X. Wen, Hamiltonian-preserving schemes for the Liouville equation with discontinuous potentials, Commun. Math. Sci., 3 (2005), 285–315.
[4] S. Jin and X. Wen, Hamiltonian preserving schemes for the Liouville equation of geometrical optics with discontinuous local wave speeds, J. Comput. Phys., 214 (2006), 672–697.
[5] S. Jin and X. Wen, A Hamiltonian-preserving scheme for the Liouville equation of geometrical optics with partial transmissons and reflections, SIAM J. Numer. Anal., 44 (2006), 1801–1828.
[6] S. Jin and X. Wen, Computation of transmissions and reflections in geometrical optics via the reduced Liouville equation, Wave Motion, 43 (2006), 667–688.

[7] S. Jin and D. Yin, Computational high frequency waves through curved interfaces via the Liouville equation and geometric theory of diffraction, J. Comput. Phys., 227 (2008), 6106–6139.
[8] Lawrence E. Kinsler, Austin R. Frey, Alan B. Coppens and James V. Sanders, Fundamentals of Acoustics, 4th Edition, Wiley, 2000.
[9] Randall J. LeVeque, Numerical Methods for Conservation Laws, Birkhäuser Verlag, 1990.
[10] J. Miklowitz, The Theory of Elastic Waves and Waveguides, North Holland, 1978.
[11] L. Miller, Refraction of high-frequency waves density by sharp interfaces and semiclassical measures at the boundary, J. Math. Pure Appl., 79 (2000), 227–269.
[12] L. V. Ryzhik, G. C. Papanicolaou and J. B. Keller, Transport equations for elastic and other waves in random media, Wave Motion, 24 (1996), 327–370.